Creep of heat-cured high-performance concrete subjected to freezing or elevated temperature

Persson, Bertil

1997

LUND UNIVERSITY

PO Box 117
221 00 Lund
+46 46-222 00 00

LUND UNIVERSITY
LUND INSTITUTE OF TECHNOLOGY
Division of Building Materials

CREEP OF HEAT-CURED HIGH-PERFORMANCE CONCRETE SUBJECTED TO FREEZING OR ELEVATED TEMPERATURE

Bertil Persson

Report TVBM-7116
September 1997

CREEP OF HEAT-CURED HIGH-PERFORMANCE CONCRETE SUBJECTED TO FREEZING OR ELEVATED TEMPERATURE

B.S.M. PERSSON
Lund Institute of Technology, Division of Building Materials, Lund, Sweden

Abstract
This article outlines an experimental and numerical study of the short-term creep of High-Performance Concrete, HPC, with sealed curing and temperature under freezing point, compared with the creep of HPC at normal and elevated temperatures. For this purpose one quality of HPC was studied at 6 different temperatures (-15, -1, 20, 30, 40 and 60 °C) over a period of 66 hours. Parallel studies of both autogenous and drying long-term creep after heat curing were carried out. New and original results and analyses of the effect of temperature related to compressive creep of HPC are presented. At -1 °C in the concrete, the loading level was as low as 25% of the ultimate loading needed to perform the creep tests properly. At -15 °C HPC withstood 40% of the ultimate loading during creep test. The study was carried out from 1992 to 1994.
Keywords: Carbonation shrinkage, creep, creep rate, elevated temperatures, freezing, heat curing, High-Performance Concrete, High-Strength Concrete, shrinkage.

1 Introduction

HPC has a 28-day 100 mm cube compressive strength exceeding 80 MPa. In a fresh state it is possible to mix, transport and cast HPC with existing methods. HPC possesses - in addition to high strength - several other favourable qualities such as low permeability and self-desiccation. The water-cement ratio, w/c, varies between 0.20 and 0.38 for HPC. Low w/c requires silica fume in the HPC and above all superplasticizer to obtain a good workability. Most often special cements are also required. The type of aggregate is important for obtaining high strength. The grading of the aggregate influences the workability. The order of mixing the material is important. Several properties of the concrete are firmly related to the water-cement ratio, such as compressive strength, internal relative humidity, hydration and compliance, ε/σ. Other properties such as Young's modulus, Poisson's ratio and the creep coefficient do not vary much as compared to normal concrete. From a practical point of view, it was of great interest to study the creep of HPC after heat curing. It was the main objective of this study to compare creep of HPC at 20 °C with creep at other temperatures.

2 Experimental

2.1 Concrete studied

Table 1 shows the properties of the aggregates and silica fumes used [1], [2]. The composition of the cement used is shown in Table 2 [3]. Table 3 provides the composition and properties of the studied concrete [3].

Table 1. Properties of aggregates and silica fumes used in present experiments [1], [2].

Type of aggregate	Elastic modulus	Compressive strength	Split tensile strength	Ignition losses
Quartzite sandstone	60.2 GPa	332 MPa	15.0 MPa	0.28%
Natural sand				0.79%
Granulated silica fume				2.26%

Table 2. Chemical composition of cement (%) [3].

Analysed properties:	
CaO	64.6
Al_2O_3	3.34
Fe_2O_3	4.39
MgO	0.84
K_2O	0.62
Na_2O	0.07
Alkali	0.48
SO_3	2.23
CO_2	0.14
Ignition losses	0.63
Free CaO	1.13
Mineralogical properties:	
C_2S	22.5
C_3S	53.0
C_3A	1.42
C_4AF	13.4
Blaine fineness	325 m^2/kg
Density	3180 kg/m^3

Table 3. Composition (kg/m^3 dry material) and properties of the concretes [3].

Material	kg/m^3 (dry material)
Quartzite sandstone 12-16 mm	1005
Natural sand 0-8 mm	765
Cement (low-alkaline)	525
Granulated silica fume	53
Superplasticizer (melamine formaldehyde)	6.4
Water-cement ratio, w/c	0.30
Air-content (% by total volume)	0.9
Density (kg/m^3)	2510
Aggregate content	0.705
Slump (mm)	230
28-day sealed cube strength (MPa)	137
1-year sealed cube strength (MPa)	144
2-year sealed cube strength (MPa)	149
4-year sealed cube strength (MPa)	139

2.2 Specimens

Cylinders 300 mm long and 55 mm in diameter were used for the creep studies. At the commencement of the tests the minimum specified specimen size was 3 times the maximum size of the aggregate. (The specimens actually taken had a diameter of 3.5 times the aggregate.) However, after the experiments began, new guidelines were introduced suggesting a minimum specimen size of 5 times the maximum aggregate [4]. No evidence was found to support the so-called skin effect of the specimen, affecting basic creep with a smaller cross- section [5]. The size of the specimen was chosen to avoid temperature effects on the deformations at early ages. Hydration, self-desiccation, and strength were studied on 100 mm cubes. Strength tests were also conducted on cylinders of the same size as those used in the creep tests. Table 4 shows a summary of the size and numbers of specimens used in the experiments [6].

Table 4 - A summary of the size and numbers of specimens used in the experiments [6].

Parameter	Cylinder 55x300 mm	Cube 100 mm
Short-term creep	12	
Long-term creep	6	
Autogenous shrinkage	12	
Compressive strength	4	72
Internal relative humidity		72
Hydration		72

The following steps were followed to mix and cast the concrete [6]:

1. The moisture of the gravel was 4%, which was accounted for in the calculations of w/c.
2. All materials except water, air-entraining agent, and superplasticizer were mixed for 30 s.
3. The water and air-entraining agent were added and mixed for another 30 s.
4. Finally, superplasticizer was added and mixed for another 3 minutes.

5. The concrete was cast in steel moulds (cylinders or cubes) and vibrated for 30 s.
6. The specimens were cured sealed at a constant temperature of 20 °C (the maximum rise of temperature internally of the concrete was 4 °C, which was measured by a thermo couple).
7. After 16 h the specimens were demolded and sealed with 2 mm vulcanized butyl-rubber.
8. Items cast-in in the concrete were connected to the measurement devices items on three sides of the specimen with steel-bolts through the sealing of butyl rubber.
9. Initial measurements were taken within 1 h after demoulding.

2.3 Experimental procedures

The HPC given in Table 3 was studied at various temperatures, Figure 1. The temperature during the first day was chosen to reflect a curing period in a large HPC structure. After the first day the HPC was studied at different temperatures of interest. The tested HPC cylinder was built into a climate box within an MTS machine. The loading and unloading procedures was quasi-instantaneous during the short-term studies in the MTS machine [6]. The HPC was cured at about 48 °C for 16 h and then tested at various temperatures, Figure 1.

The loading on the HPC cylinders was applied at 1 day's age. The cylinders were unloaded after 66 h. Parallel to the tests in the MTS machine long-term tests of heated HPC were performed. The first day of curing of the long-term tests was carried out at about 48 °C Figure 1. The HPC was then studied at 32 °C for 66 h. The creep devices were placed in same climate chamber as was supplying the MTS machine, i.e. the same temperature was obtained in the specimen at the short-term and at the beginning of the long-term tests. After the early curing at 48 °C for 1 day and the short-term curing at 32 °C for 2.7 days the creep of the cylinders was studied at 20 °C, sealed or air cured, for more than 1000 days.

3 Results of short-term creep

The climate chamber that was used to maintain the relative humidity and temperature in the MTS machine was connected to another chamber in which cubes of 100 mm were placed in order to study the mechanical properties of the HPC. Figure 2 gives the compressive strength. One day of heat curing reduced the strength at 28 days' age by about 10%. The heated HPCs obtained the same strength after 1 day of curing as did HPCs cured at 20 °C after about 2 days. Figures 3-5 give the hydration, internal relative humidity, IRH, and weight losses of the heated HPC. The heat-cured HPCs obtained lower relative hydration and also initially a lower IRH than the HPCs cured at normal temperature, which explained the resulting lower strength at 28 days' age. Figure 6 shows the shrinkage of the HPC after heat curing according to Figure 1. Figure 7 shows the shrinkage versus the weight losses, i.e. a combination of Figures 5 and 6. Figure 8 shows the total compliance reduced by the shrinkage versus loading time at various curing temperatures. Symbols in the figures: B = sealed curing; D = air curing; T= temperature (°C).02 = batch number; (0.30) = stress/strength level at loading.

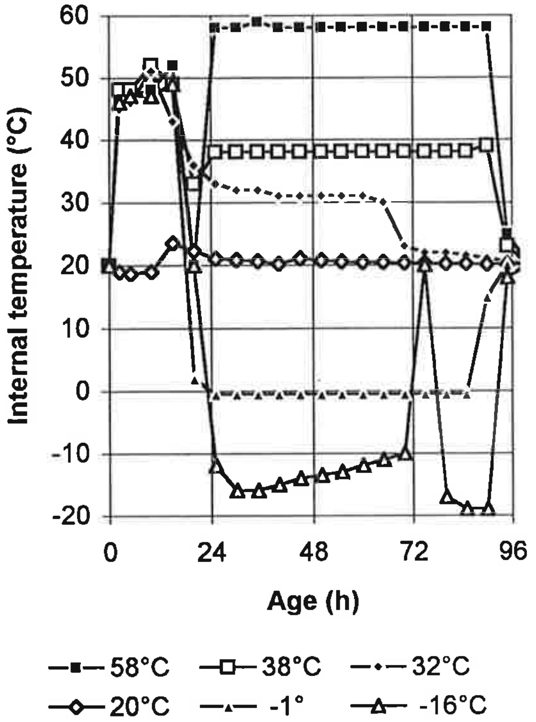

Figure 1. The HPC was cured at 48 °C for 16 h and then tested at different temperatures.

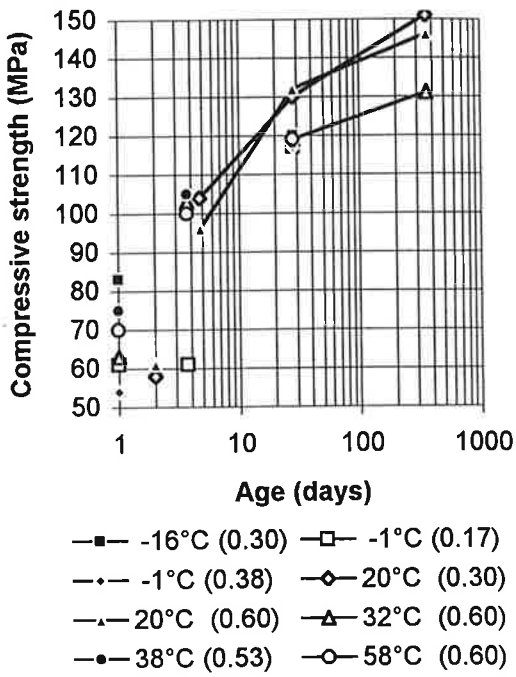

Figure 2. Strength of HPC cured at various temperatures.

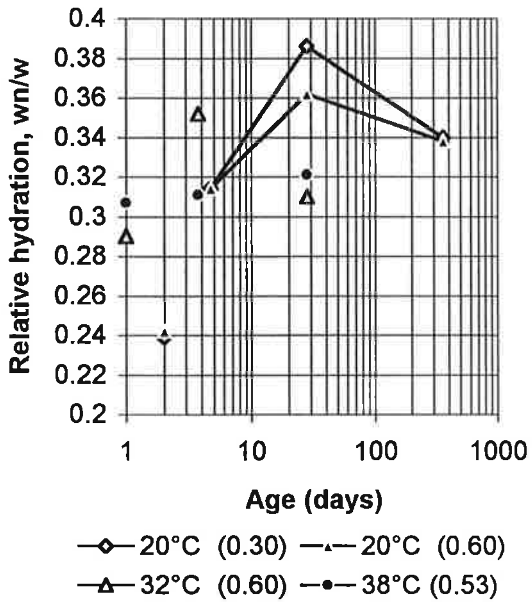

Figure 3. Relative hydration in the HPC.

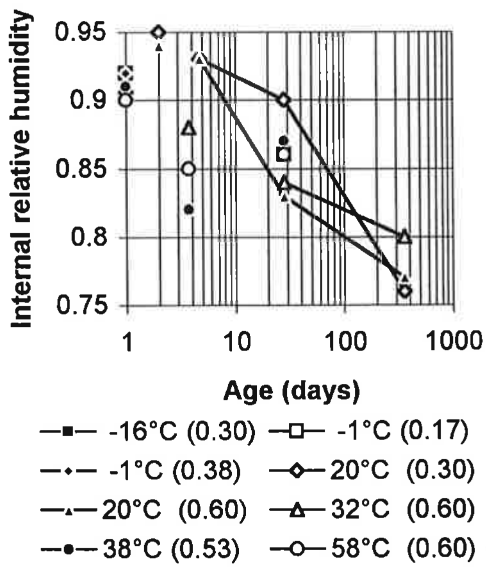

Figure 4. Relative humidity in the HPC.

Symbols: B = sealed curing; D = air curing; T= temperature (°C). 02 = batch number; (0.30) = stress/(cube strength) level at loading, i.e. stress/(cylinder strength) = 0.42.

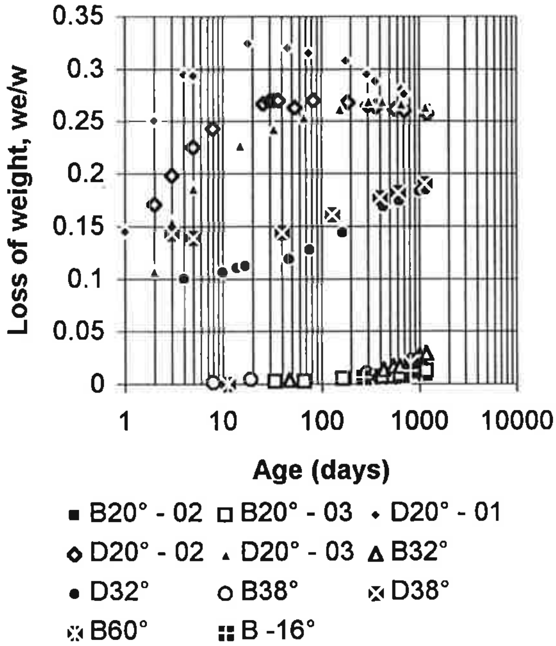

Figure 5. Weight losses of the HPC.

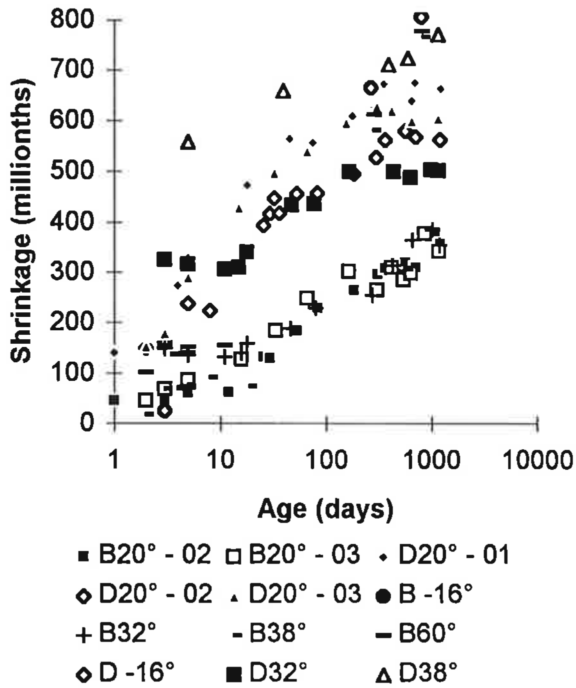

Figure 6. Shrinkage in the HPC.

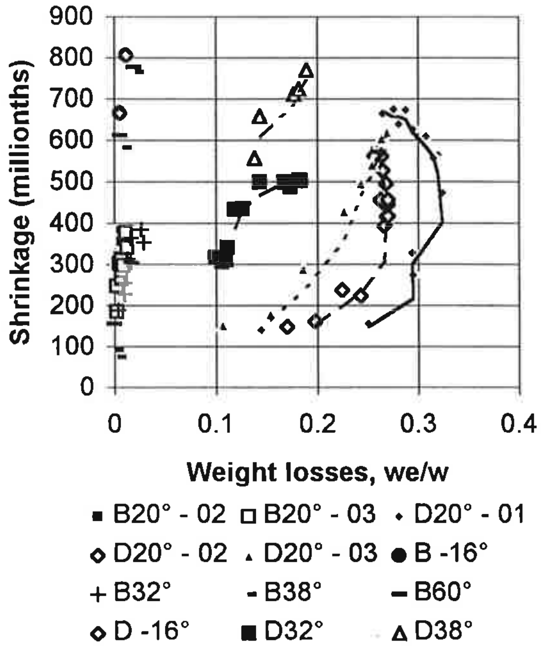

Figure 7. Shrinkage versus loss of weight.

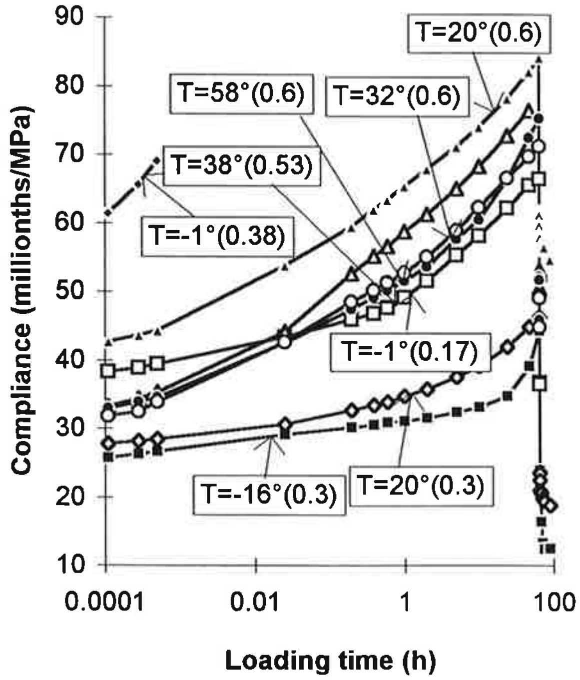

Figure 8. Reduced compliance versus time.

4 Analysis and discussion of short-term creep after heat curing

Some variations in the temperature were observed during the creep test at -16 °C. At -1 °C rapid failures of the specimens were observed both at $\sigma/f_c = 0.6$ and at $\sigma/f_c = 0.38$. At -1 °C the short-term tests only were carried out at a stress to strength ratio, $\sigma/f_c = 0.17$. Remaining tests at temperatures other than -1 °C were carried out at $\sigma/f_c = 0.3$ (-16 °C) or at $\sigma/f_c \approx 0.6$ (32°, 38° and 58 °C). As a reference creep results from the HPC cured at 20 °C and loaded at 1 and 2 days' age are shown in Figure 8. The failures of the specimens at -1 °C were probably due to formation of some salts only stable at this temperature [7-9]. However, more research is required to confirm this hypothetical failure mechanism that occurred during creep tests of HPC at -1 °C only. Figure 9 shows the creep rate versus the stress to strength ratio at loading. The creep rate versus the temperature of the specimen is shown in Figure 10. The creep rate of HPC at -1 °C was substantially larger than at other temperatures.

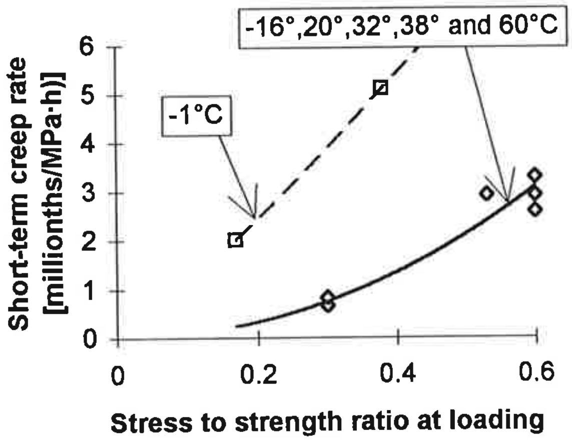

Figure 9. Creep rate of heated HPC versus the stress to strength ratio at loading.

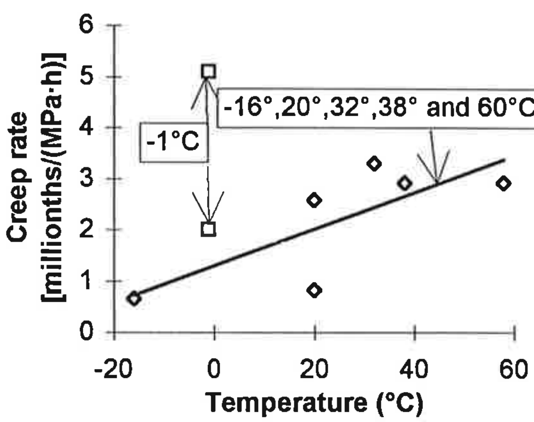

Figure 10. Short-term creep rate versus the temperature of the specimen.

The following equations of the creep rate were calculated:

$\delta J/\delta t = [8.8/(t-t')]\cdot(\sigma/f_c)^2$ $\{0.30<\cdot(\sigma/f_c)<0.60$ except for T= -1 °C$\}$ (1)

$(\delta J/\delta t)_{-1°} = [16/(t-t')]\cdot(\sigma/f_c)^{1.16}$ $\{0.17<(\sigma/f_c)<0.38\}$ (2)

$\delta J/\delta t = [0.036/(t-t')]\cdot(T+36)$ $\{-20<T<60$ °C except for T= -1 °C $\}$ (3)

Symbols in Figures 8-9 and in equations 1- 3:

f_c	denotes the compressive cube strength when loading the HPC (MPa)
$(\delta J/\delta t)_{-1°}$	denotes the creep rate of HPC at -1 °C [millionths/(MPa·h)]
$\delta J/\delta t$	denotes the creep rate at -16°, 20°, 32°, 38° and 58 °C (millionths/MPa·h)
T	denotes the temperature of the HPC {-20 < T < 60 °C}
σ	denotes the stress in the HPC during the creep tests (MPa)

According to the results the stress/strength ratio at loading turned out to be more important related to the creep rate than the temperature did. The effect of temperature shown in Figure 10 was related to different stress/strength levels at loading. At 20 °C, for example, the study was carried out both at stress/strength = 0.3 and =0.6 at loading. The creep rate rose accordingly.

5 Analysis and discussion of long-term deformation after heat curing

After 1 day of heat curing at 48 °C the curing was carried out at 32 °C for 2.7 days, both related to long-term creep and shrinkage. During the short-term creep test in the MTS machine parallel long-term test were started up in a climate chamber with exactly the same climate as in the MTS machine. However, during the first 2.7 days only an initial temperature of 32 °C was studied regarding long-term deformations. After this period the creep studies were carried out at 20 °C for more than 1000 days. Figure 2 shows the long-term strength of the HPC, i.e. about 13% lower strength after 1 year and heat curing compared to curing at 20 °C. The lower hydration after heat curing partly expressed the lower strength, cp. Figures 2 and 3. Another explanation for the lower strength after heat curing was the lower IRH, Figure 4. At both 4 and 28 days' age the IRH was about 5% lower after heat curing than after curing at 20 °C, leaving less water in the HPC available for development of hydration and strength [10].

The long-term weight losses were substantially lower after heat curing at 48 °C than after curing at 20 °C, Figure 5. Moreover HPC cured at 20 °C started to increase in weight after above 28 days' age, probably due to carbonation [11]. No such increase of weight was observed after heated curing of HPC, probably indicating that no carbonation occurred. The heat curing probably created a more dense surface of HPC which delayed the transport of carbondioxide or, alternatively, the surface of HPC obtained too a low relative humidity for carbonation to occur. Less drying occurred in heat-cured HPC than in HPC cured at 20 °C: about 20% of the mixing water evaporated from the heated HPC over 1000 days but about 25% of the amount of mixing water from HPC cured at 20 °C. Figure 7 confirms these results. In order to study the shrinkage after heated curing it was essential to know the coefficient of thermal dilatation at various temperatures. Figure 11 shows that the coefficient of thermal dilatation as an average was found to be about 0.01 per mil/ °C although slightly increasing with the temperature. From Figure 11 the following coefficient of thermal dilatation was obtained:

$$\alpha_T = (9.8+0.014\cdot\Delta T) \qquad \{-20 < T < 60\ °C\} \qquad (4)$$

α_T denotes the coefficient of thermal dilatation $\{m\cdot 10^{-6}/(m\cdot °C)\}$

ΔT denotes the change in temperature (°C)

The long-term autogenous shrinkage over 1000 days was about 0.35 per mil after curing at 20 °C but twice as large after heat curing (about 0.7 per mil), Figure 7. The reason for this observation is unknown. Figure 7 also shows that the drying shrinkage over 1000 days was about 0.6 per mil after curing at 20 °C and about 0.7 per mil after heat curing, results which coincided well with the correlations presented in chapter 8 above. The long-term reduced creep compliance is shown in Figure 12. (The shrinkage strain was reduced from the creep strain.) The creep rate with sealed curing increased with the increase of curing temperature, Table 5, which coincides well with Figure 10. However, the opposite effect of the temperature was observed with air curing, Table 5. Then the creep rate decreased after heat curing mainly due to the different amount of evaporable water. About 19% of the mixing water evaporated from the heated HPC over 1000 days and about 26% from HPC cured at 20 °C. The driving force for drying shrinkage is evaporation of water, i.e. decrease of IRH, which in turn decreases the underpressure in the pore water, Figure 13. Since the IRH decreased much more in the 20 °C-cured specimen a larger creep rate also was observed. The creep rate of heated HPC was independent of the curing condition since the decrease of IRH was of the same order for the two curing conditions.

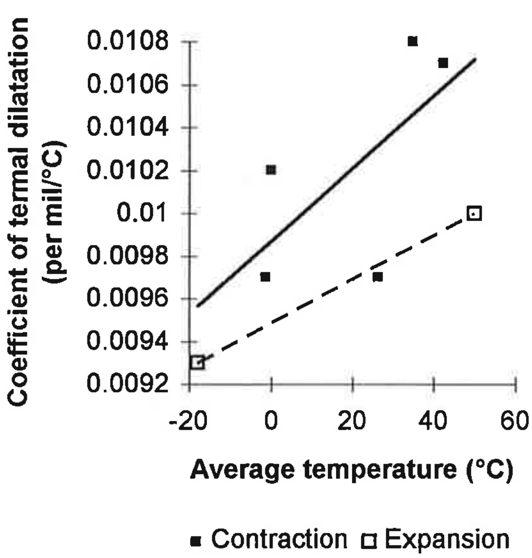

Figure 11. Coefficient of thermal dilatation versus the average internal temperature.

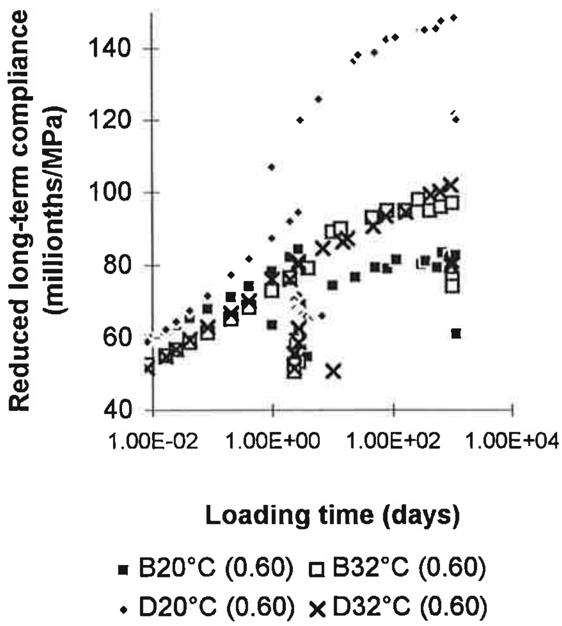

Figure 12. Reduced long-term versus the loading time.

Table 5. Reduced long-term creep rate {millionths/(days·MPa)}

Conditions	**Cured at 20 °C**	**Heat-cured**
Basic creep	2.1	3.8
Drying creep	7	3.9

6 Summary and conclusion

Short-term creep of HPC with w/c = 0.30 was studied at temperatures varying between -16 and 58 °C. The rate of creep was correlated to the temperature except for -1 °C at which temperature rapid failures were observed during the creep tests, probably due to the formation of salts in the HPC. The salts were only stable at this particular

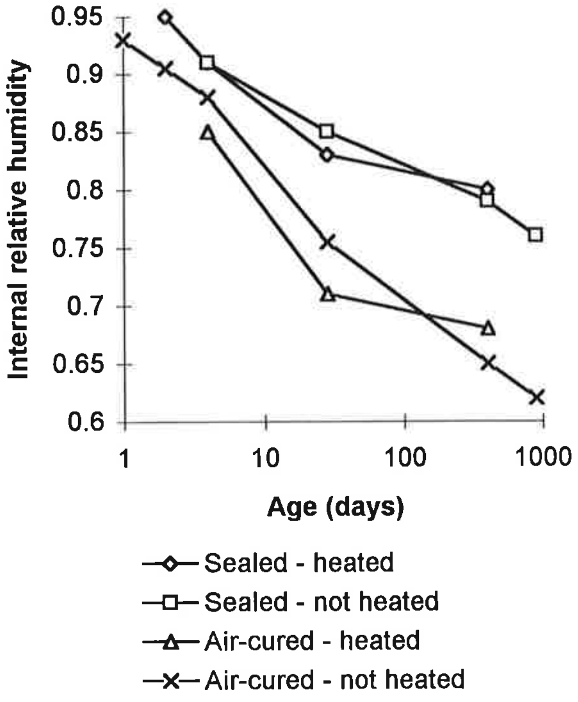

Figure 13. Internal relative humidity of long-term creep tests related to ambient curing.

temperature. This hypothesis still has to be confirmed by further research. Long-term creep of HPC after heat curing was studied for more than 1000 days. Parallel studies were carried out related to strength, hydration, internal relative humidity weight losses and shrinkage. It was the main objective of this study to compare creep of HPC at 20 °C with creep at other temperatures. The following conclusions were drawn:

1) The creep rate of HPC during short-term creep increased both with the stress to strength ratio and with the temperature. Much larger creep rate was observed at -1 °C than at other temperatures with the stress to strength ratio held constant.
2) The long-term creep rate with sealed curing also increased with the increase of curing temperature, which coincided well with the findings at short-term creep tests. The opposite effect of the temperature was observed with air curing since the creep rate decreased after heat curing mainly due to the different amount of evaporable water.
3) The long-term autogenous shrinkage over 1000 days was about 0.35 per mil after curing at 20 °C but twice as large after heat curing (about 0.7 per mil). The drying shrinkage over 1000 days was about 0.6 per mil after curing at 20 °C and about 0.7 per mil after heat curing, results which coincided well with shrinkage at 20 °C.

7 Acknowledgement

The study was financed by a Norwegian-Swedish Consortium for HPC (Cementa, Elkem, Euroc Beton, NCC Bygg, SKANSKA, Strängbetong, BFR, NUTEK) which is gratefully acknowledged.

8 References

1. Hassanzadeh M. (1994) Fracture Mechanical Properties of High-Performance Concrete, Report M4:05, Div. Building Materials, Lund Institute of Technology, Lund, pp. 9-14.

2. Persson, B. (1997) Self-Desiccation and Its Importance in Concrete Technology. *Materials and Structures,* Vol. 26, pp. 293-305.

3. Persson, B. (1996) Hydration and Strength of High-Performance Concrete, *Advanced Cement Based Materials,* Vol. 3, pp. 107-123.

4. Acker, P. (1993) Recommendation for measurement of time-dependent strains of concrete loaded in compression. *Proceedings of the Fifth International RILEM Symposium* (E&FN Spon, London), pp. 849-858.

5. Schneider, U. (1995) Choice of specimen size. Personal information, Weimar.

6. Persson, B. (1995) Basic creep of High-Performance Concrete, Report M6:14, Div. Building Materials, Lund Institute of Technology, Lund, pp. 11-190.

7. Stark, J. (1997) Formation of unstable ettringite at 0 °C, Personal information, Weimar.

8. Stark; J and Bollmann, K. (1995) Untersuchungen zur Bildung von Oberflächenrissen in Betonfahrbahndecken. Hochschule für Architektur und Bauwesen Weimar, Bulletin 6/7, Vol. 41, (Wissenschaftige Zeichnung von Hochschule für Architektur und Bauwesen, Weimar), pp. 65-74.

9. Stark, J. (1996) Zusammenhänge zwischen Zementhydration und Dauerhaftigkeit von Beton, Hochschule für Architektur und Bauwesen Weimar, Festkolloquium am 31. Mai 1996, (Labor für Bau- und Werkstoffchemie, Siegen), pp. 5-21.

10. Persson, B and Fagerlund, G. (1995) Self-desiccation and Its Importance in Concrete Technology, Report TVBM-3075, Div. Building Materials, Lund Institute of Technology, Lund, 256 pp.

11. Persson, B. (1997) Long-term shrinkage of High-Performance Concrete, Proceedings of the 10th International Congress on the Chemistry of Cement, Gothenburg, (Edited by Justnes, H., SINTEF, Trondheim), 2ii073.